

Synthesis, Structural Characterization, Computational Study, and Catalytic Activity of Metal Complexes Based on Tetradentate Pyridine/*N*-Heterocyclic Carbene Ligand

Pei Ling Chiu, Chun-Liang Lai, Chiung-Fang Chang, Ching-Han Hu, and Hon Man Lee*

Department of Chemistry, National Changhua University of Education, Changhua, Taiwan 50058, Republic of China

Received March 23, 2005

The ligand precursor $[\text{LH}_2]^{2+} \cdot 2\text{Br}^-$ (**1**) for the bis(NHC) ligand with *N*-picolyl moieties is synthesized in 83% yield. Complexation of **1** with palladium and nickel acetates produced $[\text{PdL}]^{2+} \cdot 2\text{Br}^-$ (**2**) and $[\text{NiL}]^{2+} \cdot 2\text{Br}^-$ (**3**), respectively, in quantitative yields. Metathesis reactions of **2** and **3** with AgPF_6 give the corresponding bromide-free complexes $[\text{PdL}]^{2+} \cdot 2\text{PF}_6^-$ (**4**) and $[\text{NiL}]^{2+} \cdot 2\text{PF}_6^-$ (**5**). Complexes **2**–**4** were characterized by X-ray structural determinations, which reveal a highly twisted helical coordination of L around the metal ions. In solution, however, the tetradentate chelate ring undergoes a rapid fluxional process of ring twisting. A theoretical study confirms that the tetradentate coordination of L in **2** and **3** is energetically more favorable than the bidentate chelation mode with dangling picolyl groups. A preliminary application of $[\text{NiL}]^{2+} \cdot 2\text{Br}^-$ in Suzuki coupling of aryl halides with phenylboronic acid shows effective activity.

Introduction

N-Heterocyclic carbenes (NHC) are currently receiving much research attention for their wide applicability in coordination chemistry and catalysis.¹ Monodentate NHC ligands have demonstrated remarkable activities in palladium-catalyzed C–C coupling reactions.² Recently, research efforts have also been devoted to the synthesis of polydentate ligands based on NHC. In particular, the combination of pyridine and NHC functionalities attracts a considerable amount of interest.^{3–10} The straightforward synthetic procedures involving easily accessible *N*-substituted imidazoles and pyridine

derivatives as starting materials lead to diverse polydentate ligands, some of which have shown interesting coordination chemistry,^{3,6–8} efficient catalytic applications,^{4,5,9} and biological activities.¹⁰ For example, the tridentate pincer framework of CNC ligands has been shown to produce remarkable catalytic activities in the Heck reaction,^{9a,f} whereas a cyclophane ligand framework based on NHC and pyridine imposes interesting

* Corresponding author. Tel: +886 4 7232105, ext. 3523. Fax: +886 4 7211190. E-mail: leehm@cc.ncue.edu.tw.

(1) For reviews, see for example: (a) Bourisou, D.; Guerret, O.; Gabbai, F. P.; Bertrand, G. *Chem. Rev.* **2000**, *100*, 39. (b) Jafarpour, L.; Nolan, S. P. *J. Organomet. Chem.* **2001**, *617–618*, 17. (c) Herrmann, W. A. *Angew. Chem. Int. Ed.* **2002**, *41*, 1290. (d) Hillier, A. C.; Grasa, G. A.; Viciu, M. S.; Lee, H. M.; Yang, C.; Nolan, S. P. *J. Organomet. Chem.* **2002**, *653*, 69. (e) Perry, M. C.; Burgess, K. *Tetrahedron: Asymmetry* **2003**, *14*, 951.

(2) (a) Zhang, C.; Huang, J.; Trudell, M. L.; Nolan, S. P. *J. Org. Chem.* **1999**, *64*, 3804. (b) Böhm, V. P. W.; Gstöttmayr, C. W. K.; Weskamp, T.; Herrmann, W. A. *J. Organomet. Chem.* **2000**, *595*, 186. (c) Viciu, M. S.; Germaineau, R. F.; Navarro-Fernandez, O.; Stevens, E. D.; Nolan, S. P. *Organometallics* **2002**, *21*, 5470.

(3) (a) Tulloch, A. A. D.; Danopoulos, A. A.; Winston, S.; Kleinhenz, S.; Eastham, G. J. *Chem. Soc., Dalton Trans.* **2000**, 4499. (b) Gründemann, S.; Kovacevic, A.; Albrecht, M.; Faller, J. W.; Crabtree, R. H. *Chem. Commun.* **2001**, 2274. (c) Gründemann, S.; Kovacevic, A.; Albrecht, M.; Faller, J. W.; Crabtree, R. H. *J. Am. Chem. Soc.* **2002**, *124*, 10473. (d) Gründemann, S.; Albrecht, M.; Kovacevic, A.; Faller, J. W.; Crabtree, R. H. *J. Chem. Soc., Dalton Trans.* **2002**, 2163. (e) Winston, S.; Stylianides, N.; Tulloch, A. A. D.; Wright, J. A.; Danopoulos, A. A. *Polyhedron* **2004**, *23*, 2813.

(4) (a) McGuinness, D. S.; Cavell, K. J. *Organometallics* **2000**, *19*, 741. (b) Wang, X.; Liu, S.; Jin, G.-X. *Organometallics* **2004**, *23*, 6002.

(5) Magill, A. M.; McGuinness, D. S.; Cavell, K. J.; Britovsek, G. J. P.; Gibson, V. C.; White, A. J. P.; Williams, D. J.; White, A. H.; Skelton, B. W. *J. Organomet. Chem.* **2001**, *617–618*, 546.

(6) (a) Catalano, V. J.; Malwitz, M. A. *Inorg. Chem.* **2003**, *42*, 5483. (b) Catalano, V. J.; Malwitz, M. A.; Etogo, A. O. *Inorg. Chem.* **2004**, *43*, 5714. (c) Prokopchuk, E. M.; Puddephatt, R. J. *Organometallics* **2003**, *22*, 563.

(7) (a) Garrison, J. C.; Simons, R. S.; Talley, J. M.; Wesdemiotis, C.; Tessier, C. A.; Youngs, W. J. *Organometallics* **2001**, *20*, 1276. (b) Baker, M. V.; Skelton, B. W.; White, A. H.; Williams, C. C. *Organometallics* **2002**, *21*, 2674. (c) Baker, M. V.; Brown, D. H.; Haque, R. A.; Skelton, B. W.; White, A. H. *Dalton Trans.* **2004**, 3756. (d) Durmus, S.; Garrison, J. C.; Panzner, M. J.; Tessier, C. A.; Youngs, W. J. *Tetrahedron* **2005**, *61*, 97.

(8) (a) Chen, J. C. C.; Lin, I. J. B. *Organometallics* **2000**, *19*, 5113. (b) Danopoulos, A. A.; Tulloch, A. A. D.; Winston, S.; Eastham, G.; Hursthouse, M. B. *Dalton Trans.* **2003**, 1009. (c) Simons, R. S.; Custer, P.; Tessier, C. A.; Youngs, W. J. *Organometallics* **2003**, *22*, 1979. (d) Danopoulos, A. A.; Tsoureas, N.; Wright, J. A.; Light, M. E. *Organometallics* **2004**, *23*, 166. (e) Son, S. U.; Park, K. H.; Lee, Y.-S.; Kim, B. Y.; Choi, C. H.; Lah, M. S.; Jang, Y. H.; Jang, D.-J.; Chung, Y. K. *Inorg. Chem.* **2004**, *43*, 6896. (f) Danopoulos, A. A.; Wright, J. A.; Motherwell, W. B. *Chem. Commun.* **2005**, 784.

(9) (a) Gründemann, S.; Albrecht, M.; Loch, J. A.; Faller, J. W.; Crabtree, R. H. *Organometallics* **2001**, *20*, 5485. (b) Peris, E.; Loch, J. A.; Mata, J.; Crabtree, R. H. *Chem. Commun.* **2001**, 201. (c) Tulloch, A. A. D.; Danopoulos, A. A.; Tizzard, G. J.; Coles, S. J.; Hursthouse, M. B.; Hay-Motherwell, R. S.; Motherwell, W. B. *Chem. Commun.* **2001**, 1270. (d) Danopoulos, A. A.; Winston, S.; Motherwell, W. B. *Chem. Commun.* **2002**, 1376. (e) Nielsen, D. J.; Cavell, K. J.; Skelton, B. W.; White, A. H. *Inorg. Chim. Acta* **2002**, *327*, 116. (f) Loch, J. A.; Albrecht, M.; Peris, E.; Mata, J.; Faller, J. W.; Crabtree, R. H. *Organometallics* **2002**, *21*, 700. (g) Poyatos, M.; Mata, J. A.; Falomir, E.; Crabtree, R. H.; Gibson, E. *Organometallics* **2003**, *22*, 1110. (h) McGuinness, D. S.; Gibson, V. C.; Steed, J. W. *Organometallics* **2004**, *23*, 6288.

(10) Melaiye, A.; Simons, R. S.; Milsted, A.; Pingitore, F.; Wesdemiotis, C.; Tessier, C. A.; Youngs, W. J. *J. Med. Chem.* **2004**, *47*, 973.

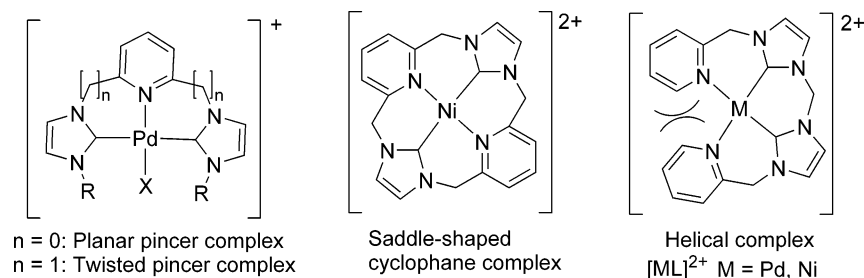


Figure 1. Metal complexes with polydentate ligands derived from NHC and pyridine.

coordination constraints resulting in the formation of a saddle-shaped nickel complex,^{7b} the structural motif of which is commonly found in metalloporphyrins (Figure 1).

Recently, we have been engaged in preparing new polydentate ligands with the incorporation of NHC and other classical donors in the ligand frameworks and exploring their potential utilities in catalytic reactions.^{11,12} In a continuation of our interest in methylene-bridged bis(NHC) ligands,¹² herein we report the synthesis of a new methylene-bridged bis(imidazolium) bromide with *N*-picolyl groups, $[\text{LH}_2]^{2+} \cdot 2\text{Br}^-$ (**1**). Our structural study indicates that the ligand **L**, from deprotonation of **1**, with dangling picolyl arms prefers tetradentate coordination around metal centers, forming complexes in a highly twisted helical fashion. A theoretical computation indeed proves that the sterically congested tetradentate chelation in both Ni and Pd systems is energetically more favorable than the bis(NHC) coordination with dangling picolyl arms, of which numerous examples of related palladium complexes exist.^{12a,b,13}

Palladium(II) complexes with mono-, bi-, and tridentate ligands are widely used as catalysts in C–C coupling reactions.¹⁴ In contrast, metal complexes with tetradentate ligands are rarely employed because of the restriction on the available coordination sites for incoming substrates. However, the more robust nature of metal complexes with tetradentate ligands can provide extra stability to the catalytic species, and in the literature polydentate ligands with hemilabile groups have been successfully applied to various catalytic reactions.¹⁵ On the other hand, there are ongoing research efforts in replacement of palladium with the cheaper nickel for the large-scale synthesis of inexpensive compounds.¹⁶ There are, however, very few reports on using nickel NHC complexes as catalysts in Suzuki

coupling.¹⁷ Herein, our preliminary application of the tetradentate nickel complex $[\text{NiL}]^{2+} \cdot 2\text{Br}^-$ in Suzuki coupling of aryl halides with phenylboronic acid has shown effective catalytic activities including aryl chlorides as substrates.

Experimental Section

General Procedure. All reactions were performed under a dry nitrogen atmosphere using standard Schlenk techniques. All solvents used were purified according to standard procedures.¹⁸ ¹H and ¹³C{¹H} NMR spectra were recorded at 300.13 and 75.48 MHz, respectively, on a Bruker AV-300 spectrometer. Chemical shifts for ¹H and ¹³C spectra were recorded in ppm relative to residual protons of CDCl₃ (¹H: δ 7.24; ¹³C: δ 77.0), DMSO-*d*₆ (¹H: δ 2.50; ¹³C: δ 39.5), CD₂Cl₂ (¹H: δ 5.32; ¹³C: δ 53.8), and DMF-*d*₇ (¹H: δ 2.73 (the more upfield Me group); ¹³C: δ 162.7 (C=O)). Elemental analyses and ESI mass spectra were performed on a Heraeus CHN-OS Rapid elemental analyzer and a Finnigan/Thermo Quest MAT 95XL, respectively, at the Instruments Center of National Chung Hsing University, Taiwan.

2-(1*H*-Imidazol-1-ylmethyl)pyridine. This compound was previously reported¹⁹ and is now prepared by a modified procedure. A mixture of 2-picolyl chloride hydrochloride (1.00 g, 6.10 mmol), imidazole (0.42 g, 6.10 mmol), and potassium hydroxide (0.98 g, 24.40 mmol) in 20 mL of THF was refluxed for 2 days. The solvent was removed completely under reduced pressure. Dichloromethane (20 mL) and water (20 mL) were added. The organic layer was thoroughly washed by shaking vigorously in a separation funnel and then washed by a fresh portion of water (20 mL). After separation, the organic layer was dried with anhydrous MgSO₄. The solution was filtered, and the removal of the solvent under reduced pressure gave an orange liquid as pure product. Yield: 0.66 g (68%). ¹H NMR (CDCl₃): δ 5.21 (s, 2H, CH₂), 6.91 (d, ³J_{HH} = 7.8 Hz, 1H, py-H3), 6.95 (s, 1H, imi-H), 7.07 (s, 1H, imi-H), 7.17–7.24 (m, 1H, py-H5), 7.57 (s, 1H, NCHN), 7.62 (t, ³J_{HH} = 7.8, 1H, py-H4), 8.55 (d, ³J_{HH} = 4.8 Hz, 1H, py-H6). ¹³C{¹H} NMR (CDCl₃): δ 51.9 (CCH₂N), 119.0; 120.7; 122.5 (imi-C, py-C), 129.3 (py-C), 136.8; 137.2 (NCHN, py-C), 149.1 (py-C), 155.6 (py-C).

1,1'-Di(2-picolyl)-3,3'-methylenediimidazolium Dibromide (1**).** A sample of 2-(1*H*-imidazol-1-ylmethyl)pyridine (2.03 g, 12.80 mmol) in 10-fold excess of methylene bromide (13 mL, 128.00 mmol) was heated at 70–80 °C for 1 day. The solvent was removed under vacuum. The residue was washed several times with THF. The hygroscopic off-white solid was filtered on a frit and dried under vacuum. Yield: 5.24 g (83%). Anal. Calcd for C₁₉H₂₀N₆Br₂: C, 46.36; H, 4.10; N, 17.07. Found: C, 46.34; H, 4.08; N, 17.01. Mp: 48–50 °C. ¹H NMR (DMSO-*d*₆): δ 5.68 (s, 4H, NCH₂C), 6.84 (s, 2H, NCH₂), 7.42

(17) (a) Steiner, G.; Krajete, A.; Kopacka, H.; Ongania, K.-H.; Wurst, K.; Preishuber-Pfluegl, P.; Bildstein, B. *Eur. J. Inorg. Chem.* **2004**, *14*, 2827. (b) Liu, J.; Robins, M. J. *Org. Lett.* **2004**, *6*, 3421.

(18) Armarego, W. L. F.; Chai, C. L. L. *Purification of Laboratory Chemicals*, 5th ed.; Elsevier Science: Burlington, 2003.

(19) Sundberg, R. J.; Mente, D. C.; Yilmaz, I.; Gupta, G. J. *Heterocycl. Chem.* **1977**, *14*, 1279.

(11) (a) Lee, H. M.; Zeng, J. Y.; Hu, C.-H.; Lee, M.-T. *Inorg. Chem.* **2004**, *43*, 6822. (b) Lee, H. M.; Chiu, P. L.; Zeng, J. Y. *Inorg. Chim. Acta* **2004**, *357*, 4313. (c) Lee, H. M.; Chiu, P. L.; Hu, C.-H.; Lai, C.-L.; Chou, Y.-C. *J. Organomet. Chem.* **2005**, *690*, 403. (d) Chiu, P. L.; Lee, H. M. *Organometallics* **2005**, *24*, 1692. (e) Lee, H. M.; Chiu, P. L. *Acta Crystallogr.* **2004**, *E60*, ml473.

(12) (a) Lee, H. M.; Lu, C. Y.; Chen, C. Y.; Chen, W. L.; Lin, H. C.; Chiu, P. L.; Cheng, P. Y. *Tetrahedron* **2004**, *60*, 5307. (b) Chiu, P. L.; Chen, C. Y.; Zeng, J. Y.; Lu, C. Y.; Lee, H. M. *J. Organomet. Chem.* **2005**, *690*, 1682. (c) Lee, H. M.; Chiu, P. L. *Acta Crystallogr.* **2004**, *E60*, ol384.

(13) (a) Herrmann, W. A.; Schwarz, J.; Gardiner, M. G. *Organometallics* **1999**, *18*, 4082. (b) Gardiner, M. G.; Herrmann, W. A.; Reisinger, C.-P.; Schwarz, J.; Spiegler, M. *J. Organomet. Chem.* **1999**, *572*, 239. (c) Lee, H. M.; Chiu, P. L. *Acta Crystallogr.* **2004**, *E60*, ml276.

(14) For a recent review, see: Brase, S.; de Meijere, A. *In Metal-Catalyzed Cross-Coupling Reactions*; Diederich, F., Stang, P. J., Eds.; Wiley-VCH: Weinheim, 1998.

(15) Braunstein, P. *J. Organomet. Chem.* **2004**, *689*, 3953.

(16) Toker, C. E.; de Vries, J. G. *Top. Catal.* **2002**, *19*, 111.

Table 1. Crystallographic Data of 1–4

	1	2	3	4
empirical formula	C ₁₉ H ₂₀ N ₆ ²⁺ ·2Br ⁻	C ₁₉ H ₁₈ N ₆ Pd ²⁺ ·2Br ⁻ ·H ₂ O	C ₁₉ H ₁₈ N ₆ Ni ²⁺ ·2Br ⁻ ·0.5H ₂ O	C ₁₉ H ₁₈ N ₆ Pd ²⁺ ·2PF ₆ ⁻
fw	492.23	614.63	557.93	726.73
cryst syst	monoclinic	monoclinic	monoclinic	monoclinic
space group	C2/c	C2/c	C2/c	P2 ₁ /n
<i>a</i> , Å	23.6789(17)	20.0487(5)	24.0943(9)	8.4644(7)
<i>b</i> , Å	4.8423(4)	13.1997(3)	11.2364(5)	20.9138(16)
<i>c</i> , Å	19.4700(14)	16.4588(4)	15.5936(6)	13.8292(8)
β, deg	117.932(3)	90.2030(10)	96.875(2)	95.217(3)
<i>V</i> , Å ³	1972.4(3)	4355.58(18)	4191.3(3)	2437.9(3)
<i>T</i> , K	150(2)	150(2)	150(2)	150(2)
<i>Z</i>	4	8	8	4
<i>D</i> _{calcd} , Mg/m ³	1.658	1.875	1.768	1.980
no. of unique data	2155	4724	6618	5444
no. of params refined	123	281	261	429
<i>R</i> ₁ ^a [<i>I</i> > 2σ(<i>I</i>)]	0.0635	0.0557	0.0673	0.0394
<i>wR</i> ₂ ^b (all data)	0.1705	0.1620	0.2001	0.1000

$$^a R_1 = \sum(|F_o| - |F_c|)/\sum|F_o|. \quad ^b wR_2 = [\sum(|F_o|^2 - |F_c|^2)^2/\sum(F_o^2)]^{1/2}.$$

(dd, ³J_{HH} = 7.5, 4.7 Hz, 2H, py-H5), 7.57 (d, ³J_{HH} = 7.5 Hz, 2H, py-H3), 7.89 (t, ³J_{HH} = 7.5 Hz, 2H, py-H4), 7.94 (s, 2H, imi-H), 8.15 (s, 2H, imi-H), 8.55 (d, ³J_{HH} = 4.7 Hz, 2H, py-H6), 9.75 (s, 2H, NCHN). ¹³C{¹H} NMR (DMSO-*d*₆): δ 53.8 (CCH₂N), 58.7 (NCH₂N), 122.6 (imi-C), 123.3 (imi-C), 124.3 (py-C), 124.4 (py-C), 138.1; 138.8 (NCHN, py-C), 150.0 (py-C), 153.3 (py-C).

{1,1'-Di(2-picoly)-3,3'-methylene-diimidazolin-2,2'-diylidene}palladium(II) Dibromide (2). A sample of **1** (244 mg, 0.50 mmol) and palladium acetate (112 mg, 0.50 mmol) in 5 mL of DMSO was heated at 50 °C for 3 h and then at 110 °C for 2 h. The solvent was removed under vacuum. The residue was washed with THF to give an air-sensitive dark yellow solid, which was filtered and dried under vacuum. Yield: 295 mg (99%). Anal. Calcd for C₁₉H₁₈N₆PdBr₂: C, 38.25; H, 3.04; N, 14.09. Found: C, 38.37; H, 3.03; N, 14.21. Mp: 140–142 °C. ¹H NMR (DMSO-*d*₆): δ 5.79 (s, 4H, NCH₂C), 6.43 (s, 2H, NCH₂N), 7.53 (virtual t, ³J_{HH} = 6.5 Hz, 2H, py-H5), 7.60–7.74 (m, 6H, py-H3, imi-H), 8.00 (virtual t, ³J_{HH} = 8.0 Hz, 2H, py-H4), 9.00 (d, ³J_{HH} = 4.8 Hz, 2H, py-H6). ¹³C{¹H} NMR (DMF-*d*₇): δ 55.4 (CCH₂N), 63.0 (NCH₂N), 122.3 (imi-C), 123.0 (imi-C), 124.5 (py-C), 124.7 (py-C), 139.3 (py-C), 152.2 (py-C), 154.6 (py-C), 155.4 (Pd-C). ESIpos-MS(DMF): *m/e* (%) 517 ([M - Br]⁺, 100).

{1,1'-Di(2-picoly)-3,3'-methylene-diimidazolin-2,2'-diylidene}nickel(II) Dibromide (3). A sample of **1** (543 mg, 1.10 mmol) and Ni(OAc)₂·4H₂O (275 mg, 1.10 mmol) in 5 mL of DMSO was heated at 50 °C for 3 h. The color of the solution changed from dark brown to orange and then greenish yellow in 30 min. The solvent was removed under vacuum. The residue was washed with THF to give a greenish-yellow solid, which was filtered and dried under vacuum. Yield: 595 mg (99%). Anal. Calcd for C₁₉H₁₈N₆NiBr₂: C, 41.58; H, 3.31; N, 15.31. Found: C, 41.62; H, 3.26; N, 15.35. Mp: 273–278 °C. ¹H NMR (DMSO-*d*₆): δ 5.83 (s, 4H, NCH₂C), 6.32 (s, 2H, NCH₂N), 7.51 (virtual t, ³J_{HH} = 6.3 Hz, 2H, py-H5), 7.76 (s, 2H, imi-H), 7.78 (s, 2H, imi-H), 7.81 (d, ³J_{HH} = 7.8 Hz, 2H, py-H3), 8.16 (virtual t, ³J_{HH} = 7.2 Hz, 2H, py-H4), 8.66 (d, ³J_{HH} = 5.4 Hz, 2H, py-H6). ¹³C{¹H} NMR (DMSO-*d*₆): δ 53.1 (CCH₂N), 62.2 (NCH₂N), 122.0 (imi-C), 124.1 (imi-C), 125.5 (py-C), 125.7 (py-C), 141.2 (py-C), 149.6 (Ni-C), 153.5 (py-C), 153.7 (py-C). ESIpos-MS(DMF): *m/e* (%) 469 ([M - Br]⁺, 100), 387 ([M - 2Br - H]⁺, 54).

{1,1'-Di(2-picoly)-3,3'-methylene-diimidazolin-2,2'-diylidene}palladium(II) Hexafluorophosphate (4). A mixture of **2** (207 mg, 0.35 mmol) and silver hexafluorophosphate (175 mg, 0.70 mmol) in 10 mL of DMF was stirred at room temperature for 2 h with exclusion of light. The fine powder of silver bromide formed was removed by centrifuge. The solvent of the supernatant solution was then completely removed under vacuum. An off-white solid was formed, which

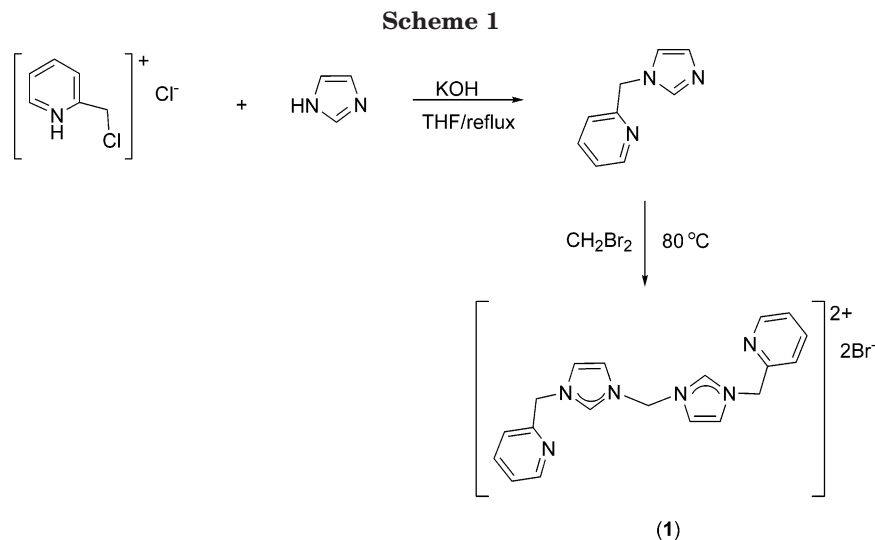
was washed with diethyl ether, filtered on a frit, and dried under vacuum. Yield: 187 mg (75%). Anal. Calcd for C₁₉H₁₈N₆-F₁₂P₂Pd: C, 31.40; H, 2.50, N, 11.56. Found: C, 31.30; H, 2.39; N, 11.29. Mp: 208–210 °C. ¹H NMR (CD₂Cl₂): δ 5.66 (s, 4H, NCH₂C), 6.42 (s, 2H, NCH₂), 7.65–7.88 (m, 8H, py-H3, py-H5, imi-H), 8.19 (t, ³J_{HH} = 7.5 Hz, 2H, py-H4), 8.84 (d, ³J_{HH} = 5.1 Hz, 2H, py-H6). ¹³C{¹H} NMR (DMSO-*d*₆): δ 54.3 (CCH₂N), 63.2 (NCH₂N), 122.7 (imi-C), 123.7 (imi-C), 126.6 (py-C), 127.0 (py-C), 141.9 (py-C), 150.9 (Pd-C), 152.3 (py-C), 153.0 (py-C).

{1,1'-Di(2-picoly)-3,3'-methylene-diimidazolin-2,2'-diylidene}nickel(II) Hexafluorophosphate (5). The complex was prepared following a procedure similar to that for **4**. A mixture of **3** (51 mg, 0.09 mmol) and silver hexafluorophosphate (47 mg, 0.19 mmol) was used. An orange solid was obtained. Yield: 49 mg (77%). Anal. Calcd for C₁₉H₁₈N₆-F₁₂P₂Ni: C, 33.61; H, 2.67; N, 12.38. Found: C, 33.51; H, 2.65; N, 12.18. Mp: 238–240 °C. ¹H NMR (CD₂Cl₂): δ 5.79 (s, 4H, NCH₂C), 6.40 (s, 2H, NCH₂), 7.56–8.23 (m, 8H, py-H3, py-H5, imi-H), 8.20 (t, ³J_{HH} = 7.1 Hz, 2H, py-H4), 8.57 (d, ³J_{HH} = 5.4 Hz, 2H, py-H6). ¹³C{¹H} NMR (DMSO-*d*₆): δ 52.9 (CCH₂N), 62.4 (NCH₂N), 122.3 (imi-C), 125.1 (imi-C), 125.8 (2 × py-C), 141.6 (py-C), 147.9 (Ni-C), 152.6 (py-C), 153.6 (py-C).

General Procedure for the Suzuki Coupling Reactions. In a typical run, a mixture of aryl halides (1.0 mmol), phenylboronic acid (1.3 mmol), K₃PO₄·H₂O (2.6 mmol), and an appropriate amount of catalyst **3** (1 or 3 mol %) with or without 2 equiv of triphenylphosphine in 3 mL of toluene was stirred at 80 °C for an appropriate duration of time (6–26 h) under nitrogen. The solution was allowed to cool. A 1:1 mixture of diethyl ether/water (20 mL) was added. The organic layer was washed, separated, further washed with another 10 mL portion of diethyl ether, and dried with anhydrous MgSO₄. The solution was then filtered. The solvent and any volatiles were removed completely under high vacuum to give a crude product, which either was subjected to column chromatography or analyzed by ¹H NMR spectroscopy.

X-ray Data Collection. Crystals of **1** and **3** were obtained by vapor diffusion of diethyl ether into their corresponding DMF solution. For crystals of **2** and **4**, the solvent combinations of methanol/diethyl ether and acetonitrile/diethyl ether were used, respectively. Typically, the crystal was removed from the vial with a small amount of mother liquor and immediately coated with silicon grease on a weighing paper. A suitable crystal was mounted on a glass fiber with silicone grease and placed in the cold stream of a Bruker APEX II with graphite-monochromated Mo Kα radiation (λ = 0.71073 Å) at 150(2) K. Crystallographic data of **1–4** are listed in Table 1.

Solution and Structure Refinements. Calculations for the structures were performed using SHELXS-97 and SHELXL-97. Tables of neutral atom scattering factors, *f*' and *f*'', and



absorption coefficients are from a standard source.²⁰ All atoms except hydrogen atoms were refined anisotropically. All hydrogen atoms in **1–3** were included through the use of a riding model. All hydrogen atoms, except H(15), in **4** were located in the difference Fourier map. Crystallographic data (excluding structure factors) for the structures in this paper have been deposited with the Cambridge Crystallographic Data Centre as supplementary publication numbers CCDC 26599–26501 (**1–3**) and CCDC 275314 (**4**). Copies of the data can be obtained, free of charge, on application to CCDC, 12 Union Road, Cambridge, CB2 1EZ, UK [fax: +44(0)-1223-336033 or e-mail: deposit@ccdc.cam.ac.uk].

Results and Discussion

Synthesis and Characterization of Ligand Precursors 1. The title ligand precursor, 1,1'-di(2-picolyl)-3,3'-methylenediimidazolium dibromide, $[\text{LH}_2]^{2+} \cdot 2\text{Br}^-$ (**1**), was prepared following our developed procedure of similar compounds.^{12a} Hence, as shown in Scheme 1, the quaternization of 2-(1*H*-imidazol-1-ylmethyl)pyridine with neat methylene bromide at 70–80 °C for 1 day and the subsequent removal of solvent and precipitation with THF produced **1** as an off-white solid in good yield (83%). The new imidazolium bromide obtained is highly hygroscopic. It is not soluble in dichloromethane and chloroform but dissolves readily in highly polar solvents, such as DMSO and DMF. It was characterized by ¹H and ¹³C{¹H} NMR spectroscopy as well as elemental analysis. The carbenic hydrogen in **1** observed at δ 9.74 is in the usual range of related imidazolium halides (δ 9.0–12.0).^{12a} It should be noted that the quaternization reaction is highly selective without the formation of pyridinium salt as side-product, reflecting the more nucleophilic nature of the imidazole compared with the pyridine functionality.

Structural Comments on 1. Crystals of **1** was successfully obtained by vapor diffusion of a diethyl ether solution into a DMF solution containing the ligand precursor. The molecular structure is shown in Figure 2, with its selected bond distances and angles given in the caption. The structure of **1** is solved in monoclinic space group *C2/c* with one-half of the molecular cation and a bromide anion in the asymmetric unit. The C(4)

atom is located on a crystallographic 2-fold rotation axis parallel to the *b* axis, and the corresponding symmetry operation generates the full molecular cation and the other bromide anion. The structure is essentially similar to those with *N*-(3-methoxybenzyl)^{12c} and *N*-(4-methoxybenzyl) substituents^{12a} reported recently by us. A noticeable difference between the structure of **1** and the two reported structures is that the dihedral angle between the two methylene-linked imidazole rings in **1** is 88.6°, which is significantly greater than those of 78.6° and 78.0° for the two reported structures, respectively. As depicted in Figure 3, **1** consists of extensive nonclassical hydrogen bonds of the type C–H···Br between the bromide anions and the molecular cations.

Synthesis and Characterization of Metal Complexes 2–5. Metal complexes with NHC ligands were typically prepared from imidazolium salts via the three common routes: the metal acetate protocol,²² the silver carbene transfer,²³ and the free carbene reaction.²⁴ For the preparation of divalent metal complexes with chelating bis(NHC), the acetate protocol is the method of choice because of the availability of divalent metal acetate and the subsequent formation of stable divalent metal complexes of bis(NHC). Following our previous procedure of related compounds,^{12a} heating a mixture of **1** with palladium- and nickel-acetate in DMSO for 2–5 h affords the corresponding complexes of **L** in quantitative yields (Scheme 2). The reaction time required for **2** and **3** is significantly shorter than that employed for the nickel complex of pyridine/NHC cyclophane, which requires a prolonged heating for 3 days.^{7b} The palladium complex **2** is an air-sensitive dark yellow solid, whereas the nickel complex **3**, having a better air stability, is greenish-yellow in color. Both are insoluble in common organic solvents but dissolve readily in DMF and DMSO. Notably, even though the

(21) Baker, M. V.; Brown, D. H.; Haque, R. A.; Skelton, B. W.; White, A. H. *Dalton Trans.* **2004**, 3756.

(22) Herrmann, W. A.; Elison, M.; Fischer, J.; Köcher, C.; Artus, G. R. *J. Angew. Chem., Int. Ed. Engl.* **1995**, *34*, 2371.

(23) (a) Wang, H. M. J.; Lin, I. J. B. *Organometallics* **1998**, *17*, 972. (b) Bildstein, B.; Malaun, M.; Kopacka, H.; Wurst, K.; Mitterböck, M.; Ongania, K.-H.; Opromolla, G.; Zanello, P. *Organometallics* **1999**, *18*, 4325.

(24) (a) Arduengo, A. J., III; Dias, H. V. R.; Harlow, R. L.; Kline, M. *J. Am. Chem. Soc.* **1992**, *114*, 5530. (b) Kernbach, U.; Ramm, M.; Luger, P.; Fehlhammer, W. P. *Angew. Chem., Int. Ed. Engl.* **1996**, *35*, 310.

(20) Sutton, L. E. *Tables of Interatomic Distances and Configurations in Molecules and Ions*; Chemical Society Publications: UK, 1965.

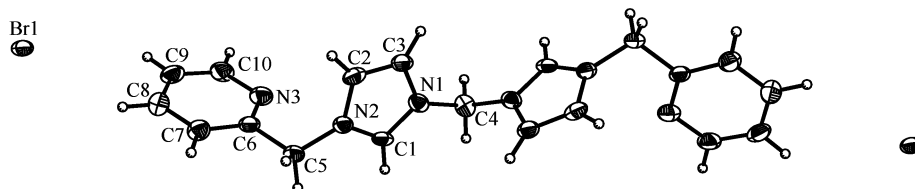


Figure 2. Thermal ellipsoid plot of **1** at the 50% probability level. Selected bond distances (Å): N(1)–C(1), 1.326(6); N(2)–C(1), 1.326(6); C(2)–C(3), 1.341(7). Selected bond angles (deg): N(1)–C(1)–N(2), 109.1(4); C(3)–N(1)–C(1), 108.5(4); C(2)–N(2)–C(1), 108.5(4); N(2)–C(2)–C(3), 107.0(4); N(1)–C(3)–C(2), 106.9(4).

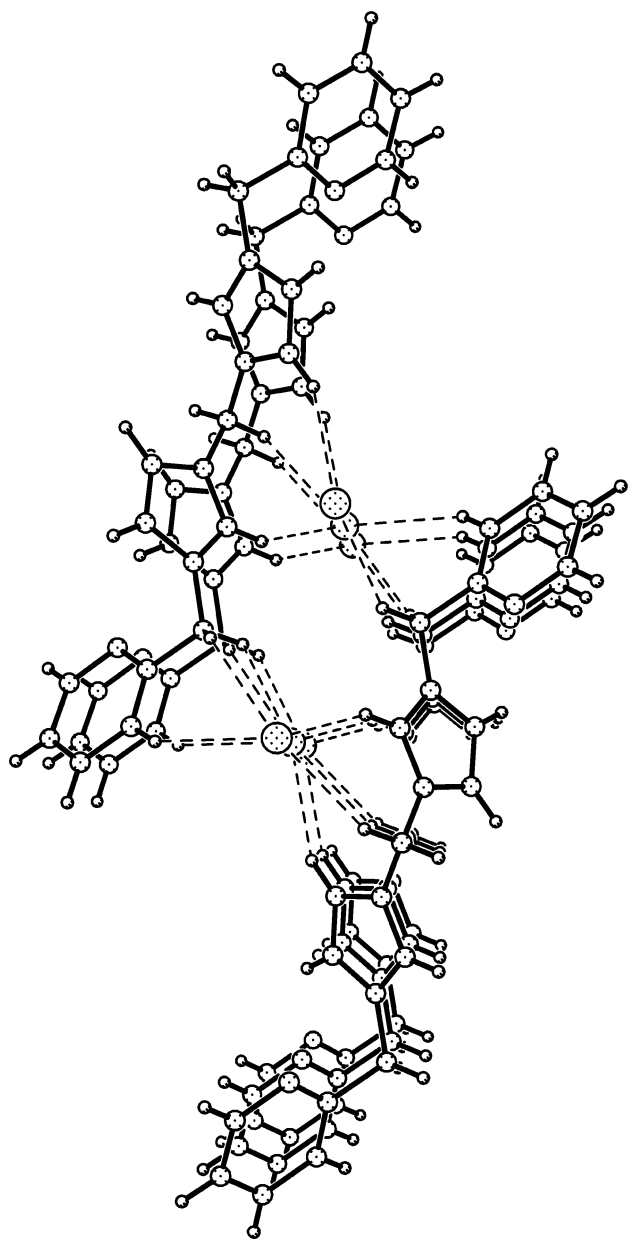


Figure 3. View of the packing of **1**, showing the hydrogen contacts between the molecular cations and bromide anions (dashed lines).

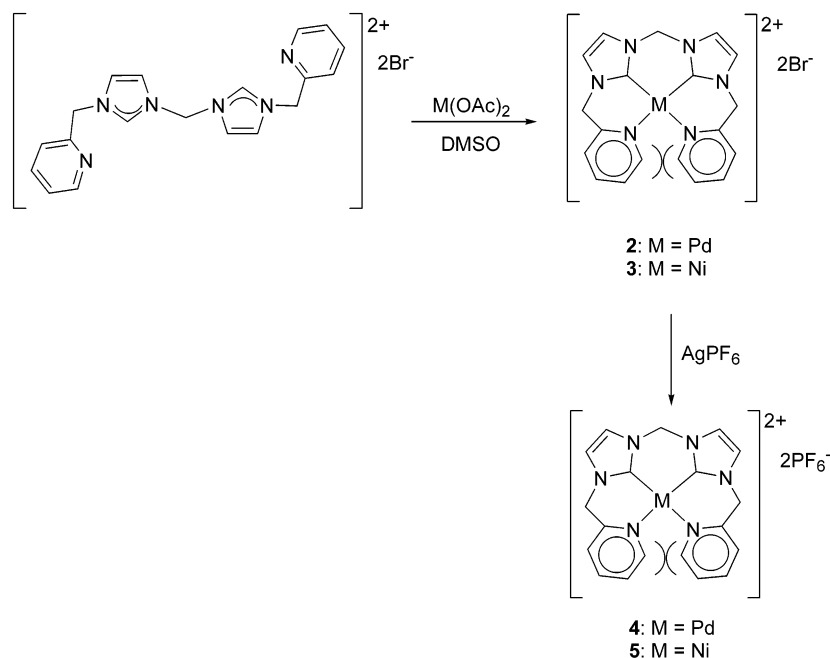
silver carbene transfer reaction is a commonly employed method for the preparation of metal complexes of NHC,²² our attempts following this route were unsuccessful.

Both ¹H NMR spectra for **2** and **3** in DMSO-*d*₆ consist of sharp signals at ambient temperature. The absence of a carbene proton at ca. 9.8 indicates the successful formation of chelating bis(NHC) complexes. In the ¹³C-

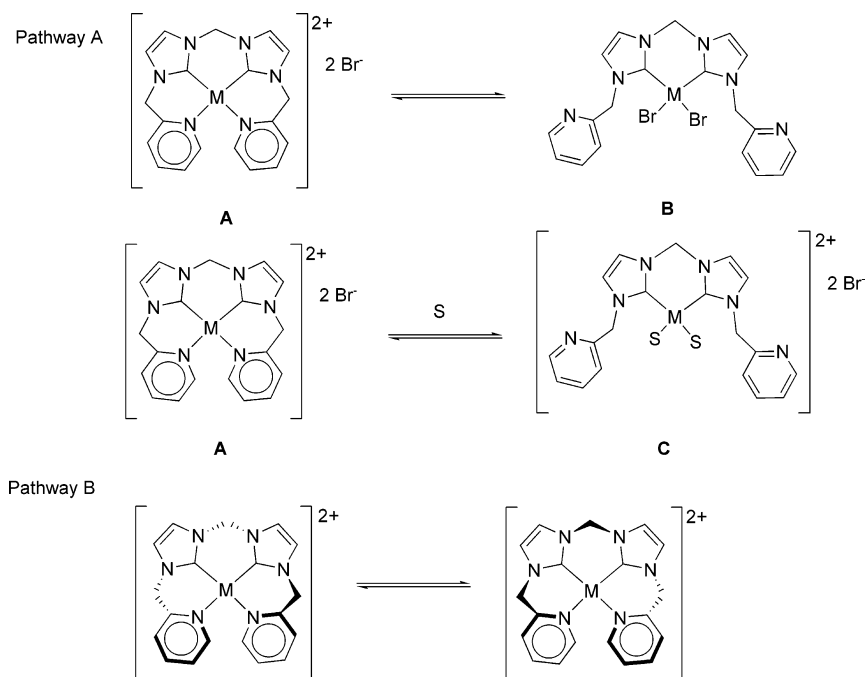
{¹H} NMR spectrum, the Pd–C resonance in **2** is detected at δ 155.4 in DMF-*d*₇, whereas the corresponding signal in **3** appears at δ 149.6 in DMSO-*d*₆. The appearance of only one set of signals for the picolyl groups and imidazole ring protons in both **2** and **3** indicates that their solution structures are symmetry-related. We have shown previously that related ligands with methylene-bridged bis(NHC) bearing noncoordinating *N*-benzyl/naphthylmethyl arms (L') form robust neutral complexes of the type PdLX₂.^{12a} However, since L contains coordinating picolyl groups, whether **2** and **3** are ionic [ML]²⁺·2Br[−] (A), with L chelated in a tetradentate fashion, or neutral MLBr₂ (B), with dangling picolyl groups, is rather dubious to distinguish by their spectroscopic data alone. The fact that they are only soluble in highly polar solvents is not conclusive enough to suggest the ionic nature of the compounds because neutral PdLX₂ also possess similar solubility.^{12a} The general downfield shift of the pyridine signals in **2** and **3** compared with those for the ligand precursor, [LH₂]²⁺·2Br[−], seems to suggest the tetradentate chelation of L around the metal ions in solution. For both complexes, rather unexpectedly, the methylene protons linking the two imidazole rings (H') and those for the picolyl moieties (H'') are observed as two sharp singlets at ca. δ 6.4 and 5.8, respectively. This is in sharp contrast to our previous observations for PdLX₂, in which H' appeared as a multiplet, whereas H'', because of intramolecular noncovalent interaction, showed an AB splitting pattern.^{12a} For a rigid tetradentate chelation of L around the metal ions, each proton within H' and H'' is in a unique environment; hence signal splitting for H' and H'' is also expected. As an example, in the nickel complex of pyridine/NHC cyclophane, the signal for the methylene protons shows an AB splitting pattern at room temperature because of the conformational rigidity of the macrocyclic ring.^{7b} Indeed, our subsequent diffraction studies identify the tetradentate chelation of L in **2** and **3** in the solid state (vide infra). The NMR data of **2** and **3** are, however, mostly consistent with a fast exchange process in solution, which renders individual protons in the methylene groups H' and H'' chemically equivalent. The fast-exchange limit spectra of **2** and **3** at ambient temperature give the sharp proton signals. Two exchange mechanisms (Scheme 3), either a halide- or solvent-assisted exchange process (pathway A), similar to that occurring in Pd(pyimpypy) complexes,^{8a} between the tetradentate and bidentate chelation with dangling picolyl groups or a tetradentate chelate ring twisting process (pathway B), similar to that proposed in the tetradentate nickel complex of NHC/cyclophane,^{7b} are envisaged.

To probe the pathway responsible for the fluxional process, ¹H NMR spectra of a DMSO-*d*₆ solution con-

Scheme 2



Scheme 3



taining **2** or **3** in the presence of 10 equiv of NBu_4Br or NBu_4I and a trace amount of trifluoroacetic acid are acquired, which give no appreciable change of the proton signals, indicating the absence of $[\text{ML}(\text{solvent})_2]^{2+} \cdot 2\text{Br}^-$ or MLBr_2 species in solution. More conclusive evidence comes from the bromide-free complexes **4** and **5**, which are synthesized by the metathesis reactions of **2** and **3** with AgPF_6 (Scheme 2). Unlike **2** and **3**, **4** and **5** are soluble in halogenated solvents. In their $^{13}\text{C}\{^1\text{H}\}$ NMR spectra, the M–C signals for **4** and **5** appear at δ 150.9 and 147.9, respectively. Significantly, the ^1H NMR spectra of **4** and **5** in CD_2Cl_2 are essentially identical to those of **2** and **3**, and for both complexes, the signals for the methylene groups H' and H'' also appear as sharp singlets, indicating the presence of a similar

fluxional process in **4** and **5**. The noncoordinating nature of the hexafluorophosphate anion and CD_2Cl_2 solvent successfully precludes the possibility of a halide- or solvent-assisted exchange process involving $[\text{ML}(\text{anion})_2]$ (**B**) or $[\text{ML}(\text{solvent})_2]^{2+} \cdot 2\text{Br}^-$ (**C**) species. Hence, the fluxional process in **2** and **3** is most probably due to the alternative chelate ring twisting mechanism involving tetradentate chelation of L. Indeed, a theoretical computation on **2** and **3** clearly demonstrates that the tetradentate coordination of L around Pd(II) and Ni(II) ions is energetically more stable (vide infra). We also carried out low-temperature ^1H NMR measurements for **2/3** and **4/5** in $\text{DMF-}d_7$ and CD_2Cl_2 , respectively. In all the cases, signal broadening is observed at low temperature. However, separate signals cannot be obtained

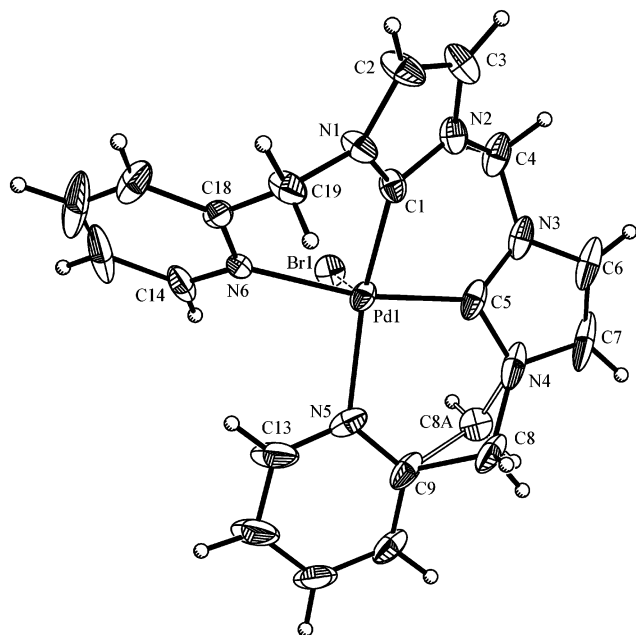


Figure 4. Thermal ellipsoid plot of the cationic portion of **2** and one of the bromide anions at the 50% probability level (one methylene group is disordered).

Table 2. Selected Bond Lengths and Angles for 2–4

	2 (M = Pd)	3 (M = Ni)	4 (M = Pd)
Bond Distances, Å			
M(1)–C(1)	2.083(4)	1.862(5)	1.955(4)
M(1)–C(5)	1.959(6)	1.862(5)	1.937(4)
M(1)–N(5)	2.133(5)	1.957(4)	2.149(3)
M(1)–N(6)	2.119(5)	1.980(5)	2.152(3)
Bond Angles, deg			
C(1)–M(1)–C(5)	85.7(3)	88.2(3)	83.76(16)
C(1)–M(1)–N(6)	85.9(2)	92.4(3)	89.15(14)
C(5)–M(1)–N(5)	90.7(3)	90.2(2)	84.59(14)
N(6)–M(1)–N(5)	99.4(2)	93.45(19)	103.10(12)
C(5)–M(1)–N(6)	167.8(3)	154.2(2)	170.65(13)
C(1)–M(1)–N(5)	167.4(2)	169.6(2)	166.59(15)
N(1)–C(1)–N(2)	105.5(5)	105.4(5)	105.9(3)

even if the samples are cooled to the low-temperature limit of their corresponding NMR solvents, indicating the rapidity of the twisting process on the NMR time scale.

Structural Comments on 2 and 4. Crystals of **2** suitable for structural analysis were obtained by the method of vapor diffusion from the solvent combination of DMF/diethyl ether. The determined structure at 150 K is shown in Figure 4, with its selected bond distances and angles tabulated in Table 2. The structure is solved in the space group $C2/c$ with a water molecule, presumably from the wet crystallization solvent, incorporated in the asymmetry unit. As depicted in the figure, the ligand L in **2** is coordinated in a tetradentate fashion with a helical structure. Because of the overlap of the two pyridine moieties, the ligand L cannot adopt a planar coordination around the palladium center. In fact, the closest separation between C(13) and C(14) on the two pyridine rings is only 3.209 Å with an anticipated strong repulsion between the hydrogen atoms upon these two carbon atoms ($H(13)\cdots H(14) = 2.200$ Å). The Pd(II) ion is in a distorted square planar coordination environment with three of the four bond angles at Pd(1) deviating significantly from the ideal 90°. The two

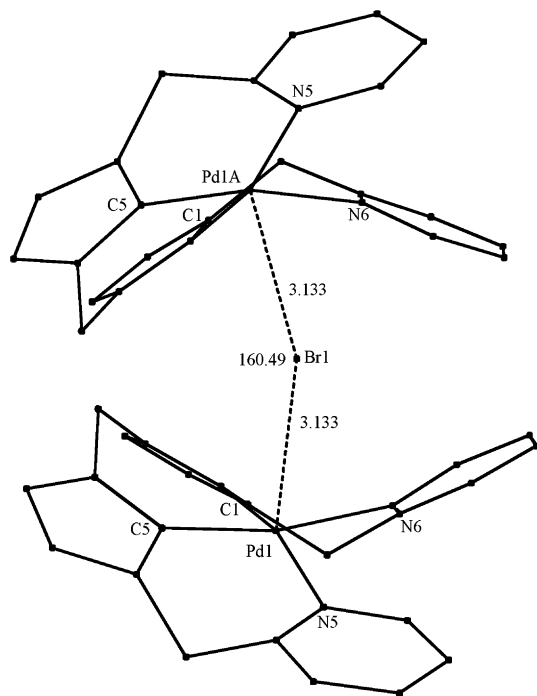


Figure 5. Perspective view of **2** showing Pd \cdots Br contacts and the helical arrangement of L (bond distance and angles are in Å and deg, respectively).

Pd–C bonds of 2.083(4) and 1.959(6) Å are slightly unequal in length, both of which are within the typical range of related compounds.^{12a} The two Pd–N bonds (2.133(5) and 2.119(5) Å) are similar in length, which, however, are markedly longer than those reported for the nickel complex of NHC/pyridine cyclophane (1.981(6) and 2.003(6) Å).^{7b} An interesting aspect of the structure is that Br(1) is involved in a nonbonding interaction of Pd \cdots Br = 3.133 Å with the palladium center at the axial position. This bromide anion is situated on a crystallographic 2-fold rotation axis parallel to the *b* axis, and the symmetry operation generates another molecular cation. Hence Br(1) is in a bridging position in close contact with two molecular cations ($\angle Pd\cdots Br\cdots Pd = 160.49^\circ$). Figure 5 is a perspective view emphasizing these Pd \cdots Br short contacts and the helical coordination of L around the palladium centers. The other bromide anions (1.5 site occupancy in total) are disordered among five general positions in the asymmetric unit. One of the methylene spacers, C(8), is also disordered among two sites.

Crystals of **4** were obtained by the method of vapor diffusion from the solvent combination of acetonitrile/diethyl ether. The thermal ellipsoid plot of the cationic portion is shown in Figure 6, with its selected bond distances and angles tabulated in Table 2. The structure is solved in the space group $P2_1/n$ with an empirical formula of $[PdL]^{2+}\cdot 2PF_6^-$ in the asymmetric unit. The ligand L, similar to that in **2**, coordinates in a helical tetradentate fashion. The Pd(1) is in a highly distorted square planar coordination geometry. Although the separation between C(13) and C(14) is 3.425 Å, which is longer than that in **2**. The separation between the hydrogen atoms upon these two carbon atoms is significantly shorter ($H(13)\cdots H(14) = 2.063$ Å). Unlike

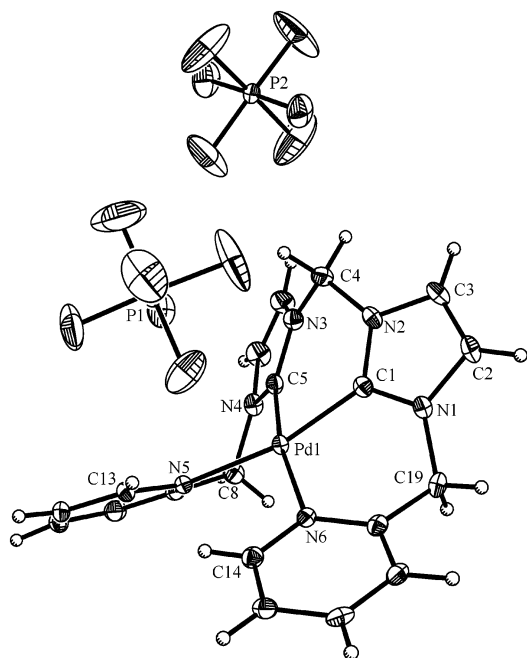


Figure 6. Thermal ellipsoid plot of **4** at the 30% probability level.

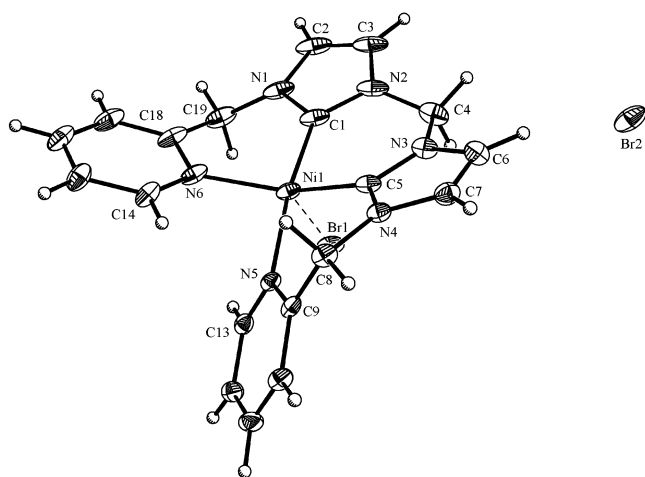


Figure 7. Thermal ellipsoid plot of **3** at the 30% probability level.

2, all of the methylene spacers are ordered and the palladium center is not interacting with the counter-anions.

Structural Comments on 3. Crystals of **3** were similarly obtained by the vapor diffusion method employed for **2**. The structure obtained at 150 K is solved in the monoclinic space group $C2/c$ with a disordered water molecule having a combined 0.5 site occupancy in its asymmetric unit. The selected bond distances and angles are tabulated in Table 2 together with those of **2** and **4**. As depicted in Figure 7, the ligand **L** in **3** also adopts a helical coordination around the metal center. The closest separation between C(13) and C(14) (3.266 Å) on the two pyridine rings is essentially similar to that of **2**. However, the H(13)⋯H(14) distance of 3.110 Å is significantly longer. The Ni(1) is distorted from the ideal square planar coordination geometry with all the four bond angles at the metal center deviating significantly from 90°. Similar to **2**, the Br(1) is also in close contact with the metal center with a shorter contact distance

of Ni(1)⋯Br(1) = 3.006 Å. However, unlike **2**, this bromide anion is in a general position and not in contact with another molecule of the cationic complex. A comparison of the bond distances around the nickel ion in **2** with those of **3** clearly reflects the smaller ionic size of the nickel ion, resulting in shorter M–C/M–N bonds.

The helical nature of the ligand **L** in **2** and **3** is best viewed in Figure 8, which is a plot showing the displacements for the 13 core atoms from the mean plane defined by the four-coordinated atoms in **2** and **3**. The maxima and minima correspond to the positions of the CH₂ carbons, suggesting the importance of flexibility of the methylene spacers as joints in maintaining the nonplanar coordination of **L**. The plot also clearly shows that **2** (the major orientation) has a more regular helical pattern than **3**. It should be noted that **2–4** adopt conformations of C_1 symmetry in their corresponding asymmetric units, whereas their solution structures are symmetry-related (vide infra). As discussed above, a ring twisting process in solution is most likely involved. The ring twisting interconversion between conformations can be represented by the two curves in Figure 8 and their corresponding mirror reflections about the x axis. Interestingly, the disorder position of C(8A) can be regarded as an indication of this twisting process. In the related palladium complex of NHC/pyridine cyclophane, a similar ring twisting process is also proposed.^{7b}

Theoretical Studies on 2 and 3. It is interesting to note the apparent sterically congested tetradentate chelation of **L** in the solid-state structures of **2** and **3** (i.e., [ML]²⁺·2Br[−] (**A**) vs MLBr₂ (**B**)). The similarity of the NMR data between the complexes consisting of bromide and PF₆[−] anions suggests the preference of tetradentate chelation of **L** in solution as well. On the other hand, methylene-linked bis(NHC) palladium halide complexes with noncoordinating *N*-substituents, Pd(NHC)₂X₂, are numerous in the literature.^{12a,b,13} Therefore, we thought it of interest to understand theoretically the relative stability between [ML]²⁺·2Br[−] (**A**) and MLBr₂ (**B**) in **2** and **3**.

We used the gradient-corrected hybrid density functional theory (DFT), B3LYP. The approach is a hybrid method, which consists of the three-parameter mixing of the nonlocal exchange functional of Becke²⁵ and correlation functional of Lee, Yang, and Parr.²⁶ During our computations we learned that the quality of basis functions is essential, especially for bromine and the metals. For Ni and nonmetal atoms, 6-31G* basis sets are used in geometry optimizations, and single-point calculations are followed using the 6-311G** basis set. For Pd, we used the basis set of Hay and Wadt²⁷ (including effective core potential), LANL2DZ, augmented with a set of functions (3s3p2d3f) that was suggested by Langhoff et al.²⁸ Solvation effects of DMSO (dielectric constant $\epsilon = 46.7$) were evaluated using the polarizable continuum model (PCM) of Cossi et al.²⁹ In this model, the solvation free energy is accounted for.

(25) Becke, A. D. *J. Chem. Phys.* **1993**, *98*, 5648.

(26) Lee, C.; Yang, W.; Parr, R. G. *Phys. Rev. B* **1988**, *37*, 785.

(27) Hay, P. J.; Wadt, W. R. *J. Chem. Phys.* **1985**, *82*, 270.

(28) Langhoff, S. R.; Pettersson, L. G. M.; Bauschlicher, C. W., Jr.; Partridge, H. *J. Chem. Phys.* **1987**, *86*, 268.

(29) Cossi, M.; Barone, V.; Cammi, R.; Tomasi, J. *Chem. Phys. Lett.* **1996**, *255*, 327.

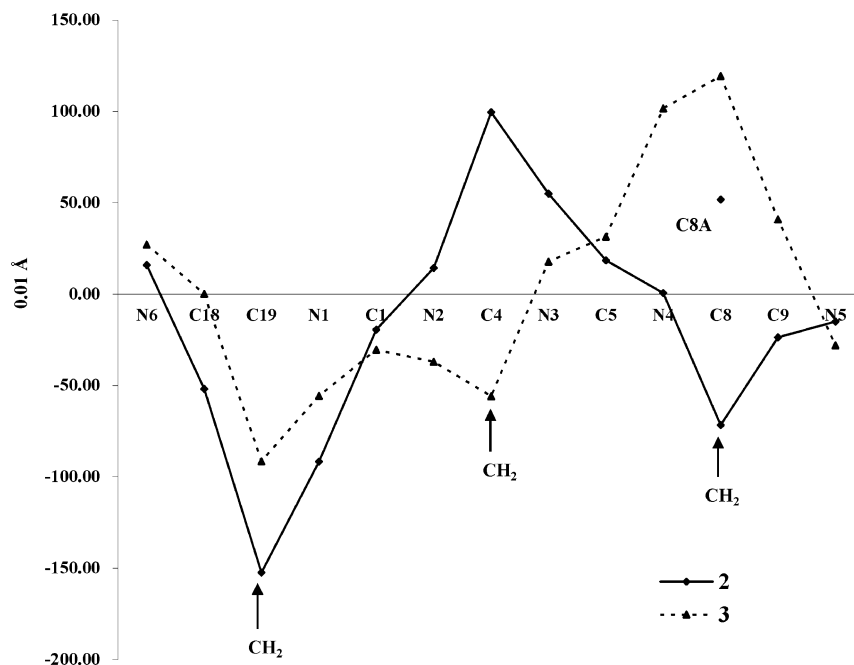


Figure 8. Plot showing the displacements for the ligand core atoms from the mean plane defined by the four coordinated atoms in **2** and **3** (C8(A) is a disorder atom in **2**).

The molecular free energy of the solute embedded in a continuum medium is computed with this method, in which the solute is polarized by the solvent, and the solute–solvent dispersion–repulsion energy is evaluated. It has been shown that the PCM model provides predictions for the free energy of hydration that are comparable with experimental results. Some of these studied species include solute–solvent hydrogen bonds, and some are ionic species.²⁹ A related polarizable conductor calculation model by Barone and Cossi (CPCM) was also applied.³⁰ All calculations were carried out using the Gaussian 03 program, Revision C.02.³¹

Our predicted structures of the $[\text{ML}]^{2+} \cdot 2\text{Br}^-$ ($\text{M} = \text{Pd}$, Ni) are in fine agreement with the solid-state structures of **2** and **3** obtained from X-ray diffraction studies. Differences between predicted bond distances are almost within 0.01 Å of the experimental data. The largest deviation is the bond distances of Pd–C, in which the predicted bond distances are approximately 0.03 Å longer. With the PCM model, the energy of reaction for MLBr_2 to form $[\text{ML}]^{2+} \cdot 2\text{Br}^-$ (plus two bromide anions) is -26.4 kcal/mol for the Ni system and -6.2 kcal/mol for the Pd system. Using CPCM, the results are -26.6 and -5.9 kcal/mol for Ni and Pd systems, respectively.

(30) Barone, V.; Cossi, M. *J. Phys. Chem. A* **1998**, *102*, 1995.

(31) Frisch, M. J.; Trucks, G. W.; Schlegel, H. B.; Scuseria, G. E.; Robb, M. A.; Cheeseman, J. R.; Montgomery, J. A., Jr.; Vreven, T.; Kudin, K. N.; Burant, J. C.; Millam, J. M.; Iyengar, S. S.; Tomasi, J.; Barone, V.; Mennucci, B.; Cossi, M.; Scalmani, G.; Rega, N.; Petersson, G. A.; Nakatsuji, T.; Hada, M.; Ehara, M.; Toyota, K.; Fukuda, R.; Hasegawa, J.; Ishida, M.; Nakajima, T.; Honda, Y.; Kitao, O.; Nakai, H.; Klene, M.; Li, X.; Knox, J. E.; Hratchian, H. P.; Cross, J. B.; Adamo, C.; Jaramillo, J.; Gomperts, R.; Stratmann, R. E.; Yazyev, O.; Austin, A. J.; Cammi, R.; Pomelli, C.; Ochterski, J. W.; Ayala, P. Y.; Morokuma, K.; Voth, G. A.; Salvador, P.; Dannenberg, J. J.; Zakrzewski, V. G.; Dapprich, S.; Daniels, A. D.; Strain, M. C.; Farkas, O.; Malick, D. K.; Rabuck, A. D.; Raghavachari, K.; Foresman, J. B.; Ortiz, J. V.; Cui, Q.; Baboul, A. G.; Clifford, S.; Cioslowski, J.; Stefanov, B. B.; Liu, G.; Liashenko, A.; Piskorz, P.; Komaromi, I.; Martin, R. L.; Fox, D. J.; Keith, T.; Al-Laham, M. A.; Peng, C. Y.; Nanayakkara, A.; Challacombe, M.; Gill, P. M. W.; Johnson, B.; Chen, W.; Wong, M. W.; Gonzalez, C.; Pople, J. A. *Gaussian 03*, Revision C.02 ed.; Gaussian, Inc.: Wallingford CT, 2004.

Hence, for both Ni and Pd systems, our computations support unequivocally that $[\text{ML}]^{2+} \cdot 2\text{Br}^-$ with L chelated in a tetradentate fashion is, especially in the case of the Ni system, energetically more favorable than MLBr_2 with dangling picolyl groups.

Suzuki Cross-Coupling. Various nickel phosphine complexes have been shown to be efficient in Suzuki cross-coupling.³² For example, $\text{NiCl}_2(\text{dppe})$ (dppe = 1,2-bisdiphenylphosphinoethane) in the presence of excess phosphine (PPh_3 or dppe) is a general catalyst for the cross-coupling of aryl mesylates, tosylates, chlorides, bromides, and iodides with arylboronic acids.^{32e} We conducted a preliminary study to determine the feasibility of using the nickel complex **3** as catalyst in the Suzuki cross-coupling between phenylboronic acid and aryl halides. We employed a similar catalytic condition reported for $\text{NiCl}_2(\text{dppe})$ ^{32e} with the use of 1–3 mol % of **3** as catalyst in the presence of 2 equiv of PPh_3 and $\text{K}_3\text{PO}_4 \cdot \text{H}_2\text{O}$ as base (Table 3). The coupling reaction is highly solvent dependent; no coupling product is obtained if 1,4-dioxane is used as solvent instead of toluene. With phenyl iodide as substrate, 1 mol % of **3** furnishes a 82% yield of biphenyl in 12 h (entries 1). The catalyst is more reactive toward activated and unactivated aryl bromides, as seen in entries 4 and 7, indicating the quantitative production of 4-acetylbiphenyl and biphenyl. However, with deactivated aryl bromide, a poor yield of 34% was obtained with 1 mol % of catalyst (entry 8). Increasing the catalyst loading to 3 mol % significantly increases the yield to 74% (entry 9). For activated aryl chloride, a high yield of 4-acetylbiphenyl (95%) is obtained with 3 mol % of catalyst in 24 h (entry 13). The catalytic system is also highly active

(32) (a) Saito, S.; Oh-tani, S.; Miyaura, N. *J. Org. Chem.* **1997**, *62*, 8024. (b) Indolese, A. *Tetrahedron Lett.* **1997**, *38*, 3513. (c) Inada, K.; Miyaura, N. *Tetrahedron* **2000**, *56*, 8657. (d) Zim, D.; Lando, V. R.; Dupont, J.; Monteiro, A. L. *Org. Lett.* **2001**, *3*, 3049. (e) Percec, V.; Golding, G. M.; Smidrkal, J.; Weichold, O. *J. Org. Chem.* **2004**, *69*, 3447. (f) Tang, Z.-Y.; Hu, Q.-S. *J. Am. Chem. Soc.* **2004**, *126*, 3058.

Table 3. Suzuki Coupling Catalyzed by $[\text{NiL}]^{2+}\cdot 2\text{Br}^-$ ^a

entry	mol % of catalyst	equiv of PPh ₃	X	R	time, h	yield, %
1	1	2	I	H	12	82 ^c
2	1		Br	COMe	6	66 ^b
3	1	2	Br	COMe	6	80 ^b
4	1	2	Br	COMe	12	100 ^b
5	3		Br	COMe	24	95 ^b
6	3	2	Br	COMe	24	100 ^b
7	3	2	Br	H	24	100 ^b
8	1	2	Br	OMe	12	34 ^b
9	3	2	Br	OMe	12	74 ^b
10	1	2	Cl	COMe	17	78 ^b
11	1	2	Cl	COMe	24	88 ^b
12	3		Cl	COMe	24	19 ^b
13	3	2	Cl	COMe	24	95 ^b
14	3		Cl	Me	24	0
15	3	2	Cl	Me	24	88 ^b
16	1	2	Cl	OMe	24	32 ^b
17	3	2	Cl	OMe	26	46 ^b

^a Reaction conditions: 1 mmol of aryl halide, 1.3 mmol of phenylboronic acid, 2.6 mmol of $\text{K}_3\text{PO}_4\cdot\text{H}_2\text{O}$ as base, 1–3 mol % of Ni catalyst, 3 mL of toluene. ^b NMR yield. ^c Isolated yield.

toward unactivated 4-chlorotoluene, which affords a 88% yield of 4-phenyltoluene (entry 15). Unfortunately, complex **3** is less efficient for deactivated aryl chloride; only a modest yield of 46% is achieved for 4-chloroanisole with a 3 mol % of catalyst loading in 26 h (entry 17). We have also briefly investigated the effect of added triphenylphosphine. For 4-bromoacetophenone, the absence of PPh_3 produced a slightly lower yield (compare entries 2 and 3; 5 and 6). The presence of PPh_3 is, however, crucial for aryl chlorides, which show a drastic reduction of yield from 95% to 19% and 88% to 0% in reactions with 4-chloroacetophenone and 4-chlorotoluene without PPh_3 added, respectively (compare entries 12 and 13; 14 and 15).

Conclusion

The imidazolium salt $[\text{LH}_2]^{2+}\cdot 2\text{Br}^-$ for the potential tetradentate bis(NHC) ligand containing *N*-picolyl groups

was synthesized. Direct reactions of $[\text{LH}_2]^{2+}\cdot 2\text{Br}^-$ with $\text{M}(\text{OAc})_2$ ($\text{M} = \text{Ni}$ and Pd) afford **2** and **3**. Since the ligand **L** contains *N*-picolyl arms, formation of either $[\text{ML}]^{2+}\cdot 2\text{Br}^-$ or MLBr_2 is possible (i.e., tetradentate vs bidentate chelation of **L**). The solid-state structures at 150 K reveal a sterically congested tetradentate chelation of **L** around the metal ions (i.e., $[\text{ML}]^{2+}\cdot 2\text{Br}^-$). Metathesis reactions of **2** and **3** with AgPF_6 give the corresponding bromide-free complexes **4** and **5**. Comparison of their ¹H NMR spectra with those of **2** and **3** also indicates the tetradentate chelation of **L** and the existence of a fast chelate ring twisting fluxional process in all these complexes in solution. Indeed, our computational studies indicate that the tetradentate chelation of **L** in $[\text{ML}]^{2+}\cdot 2\text{Br}^-$ is energetically more favorable, despite the sterically congested helical coordination of **L** around the metal ions. The use of a nickel complex with tetradentate ligand in Suzuki coupling is not known in the literature. Our initial study shows that the cationic tetradentate nickel NHC/pyridine complex **3** is, similarly to NiX_2P_2 and $\text{NiX}_2\text{P}'$ complexes (P and $\text{P}' =$ monodentate and bidentate phosphine, respectively), an efficient catalyst for Suzuki coupling reactions including aryl chlorides as substrates. Because of the stronger Ni–C than Ni–N bond, chelate ring opening from the picolyl moieties in **3** is envisaged for the catalytic activity at high temperature.

Acknowledgment. We are grateful to the National Science Council of Taiwan for financial support of this work. We also thank the National Center for High-Performance Computing for computing time and facilities.

Supporting Information Available: Full crystallographic data for compounds **1–4** are provided as a CIF file. This material is available free of charge via the Internet at <http://pubs.acs.org>.

OM050224W